1.B Absorption and Radiation of Energy from Spherically Irradiated Targets

The coupling of high-power lasers to solid matter is important to direct-drive laser fusion. Single-beam experiments at 1054 nm, 526 nm, 351 nm, and 266 nm on planar targets have shown higher absorption and lower numbers of fast electrons for shorter-wavelength laser irradiation.[1-3] It is important to determine how uniformly irradiated spherical targets couple incident laser energy. Absorption of 526-nm laser radiation, in the intensity range of 10^{14}–10^{16} W/cm^2, has been measured for spherical targets.[4] This work is a continuation of previously reported six-beam irradiation of spherical targets at 351 nm.[5] The absorption of 24 351-nm laser beams by spherical targets was measured.

This study used the 24 UV beams of the OMEGA Nd:phosphate-glass laser facility, which have been up-converted to a wavelength of 351 nm. The laser energy is focused onto spherical targets with 60-cm focal-length lenses ($f/3$) with a lateral pointing accuracy of 10 μm and an axial pointing accuracy of 50 μm. The intensity levels of the 24 beams were balanced to within 6% of each other. Tangential focus of Gaussian spatial profile beams at the energy balance stated above yield an overall variation in intensity of 20% for a 300-μm-diameter target.

The absorbed energy and x-ray radiation were determined for solid glass spheres with diameters between 90 μm and 800 μm. The laser energy was between 1.0 kJ and 1.5 kJ, with a 700-ps to 800-ps pulse width. The range of laser intensity resulting from the above conditions was 5×10^{13} to 5×10^{15} W/cm^2. All 24 beams were focused eight target radii beyond target center; marginal rays were thus tangent to the target surface. The absorbed energy was measured with a set of 15 differential plasma calorimeters symmetrically placed around the target chamber. The energy radiated into x rays was determined by a single, differential x-ray calorimeter with a solid angle of 0.26 mstr. The measured absorbed energy to laser energy and radiated energy to absorbed energy are plotted in Fig. 31.6. The absorbed energy fraction shows a larger variation over the intensity range than does the radiated energy fraction.

The scaling of absorbed energy with incident laser energy is shown in Fig. 31.7(a). The solid lines show the absorption for the experimental irradiation conditions predicted by the 1-D hydrodynamic code *LILAC*. The assumed phenomenological flux-limit parameter is $f = 0.06$. The component of absorption due to inverse bremsstrahlung is calculated using a self-consistent ray-tracing model. The beams are incident at tangential focus, as in the experiment, and the rays are traced through the 1-D refractive-index distribution, using the assumptions of geometrical optics. An additional component of absorption is included at the turning point of the ray. This small fraction ($\sim$ 15%) is included to simulate resonance absorption. Calculations omitting this additional energy are consistent with the data
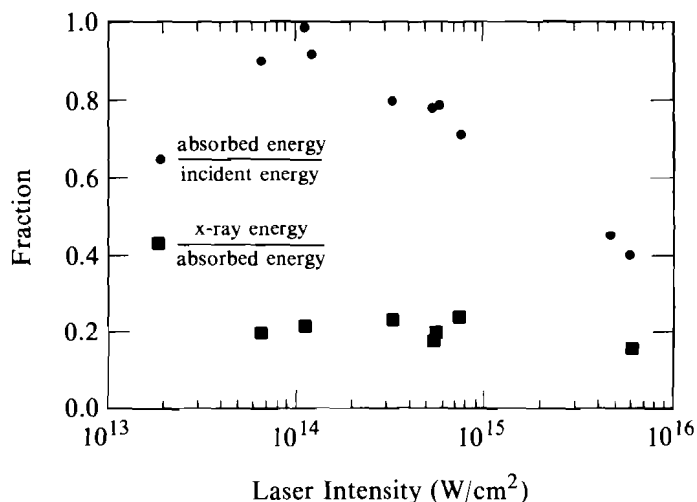
Fig. 31.6
Energy absorption versus laser intensity and radiation fraction versus laser intensity.

in the low- to mid-intensity range, but predict less absorption than is observed at intensities above 10^{15} W/cm^2. It should be noted that some resonant absorption and/or parametric decay instability occurs at 351 nm, but the energy coupled to the electrons is too low to be observed from the x-ray spectrum or to present a significant preheat problem.

Tangential-focus conditions were used in the experiment to provide good irradiation uniformity and optimum coupling of energy to the target. The solid lines in Fig. 31.7(a) show the calculation predictions for four different focusing conditions. These calculations were done for the OMEGA beam profile and for focal positions ranging from six to 12 target radii beyond the center of the target. Figure 31.7(b) shows the dependence of the absorbed-energy fraction on laser focus. The solid line is the *LILAC* prediction for an incident laser intensity of 10^{14} W/cm^2. The experimental points were measured with the same incident-laser intensity and for a laser focus range from four to eight target radii from the target center.

Because of the energy constraints, the higher illumination intensities are attained by using smaller-diameter targets. This gives rise to shorter coronal-density scale lengths and higher refractive losses. The net effect is to reduce the measured absorption. Previously reported planar target data indicate higher values of absorbed energy for intensities above mid-10^{14} W/cm^2 and 351-nm irradiation.[2] This demonstrates the effect of using smaller targets to achieve higher irradiation intensities.

It was shown in the prior measurements that the x-ray continuum spectrum for 351-nm irradiation reveals no evidence for "hot electrons" and that the "superhot electron" component is small.[5] The reported

(a)

glass
f = -0.06
f/H = 3.8
1.2 kJ
600 ps

OMEGA beam
profile

U115

Laser Intensity (W/cm^2)

(b)

glass
f = -0.06
f/H = 3.8
1.2 kJ
600 ps

Focus Position (R)
$1 \sim 10^{14}$ W/cm^2

U119
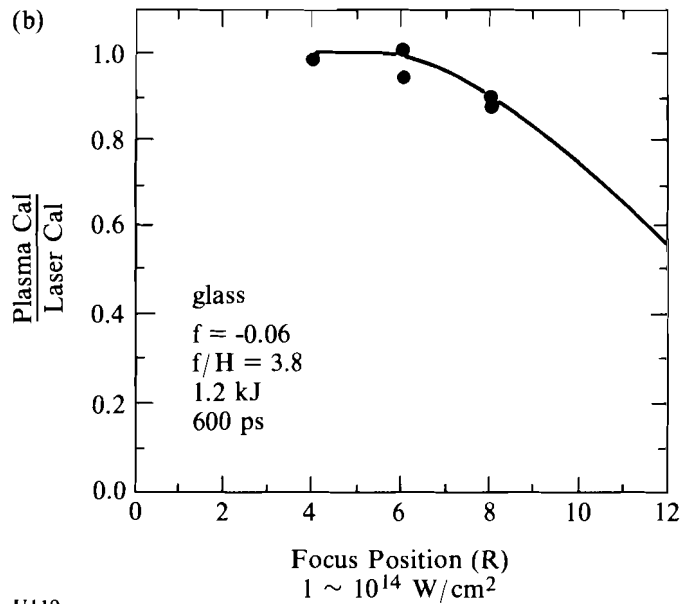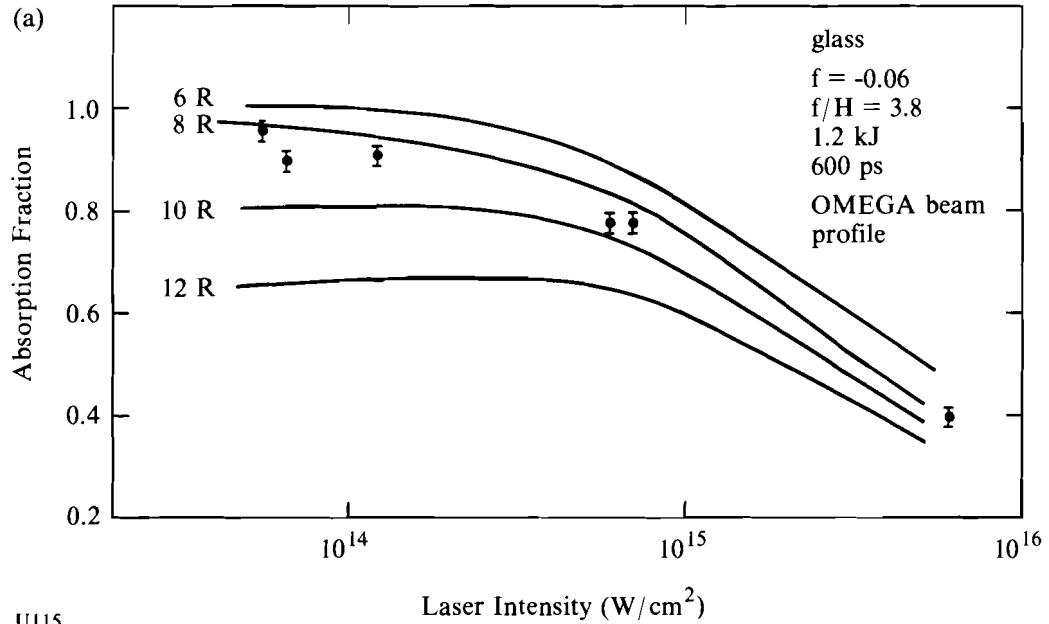
Fig. 31.7
(a) Scaling of absorption fraction;
(b) absorption.

fraction of incident energy in the superhot electrons is about 10^{-4}. It was decided to measure the total energy radiated into x rays. A differential x-ray calorimeter was constructed to make this measurement. (The sensitivity of this calorimeter is shown in Fig. 31.8.) The calorimeter has a flat sensitivity for x rays with energies less than 6 keV. At 6 keV, effects of the Ta L_3 absorption edge at 9.877 keV are evident. This detector is insensitive to the superhot
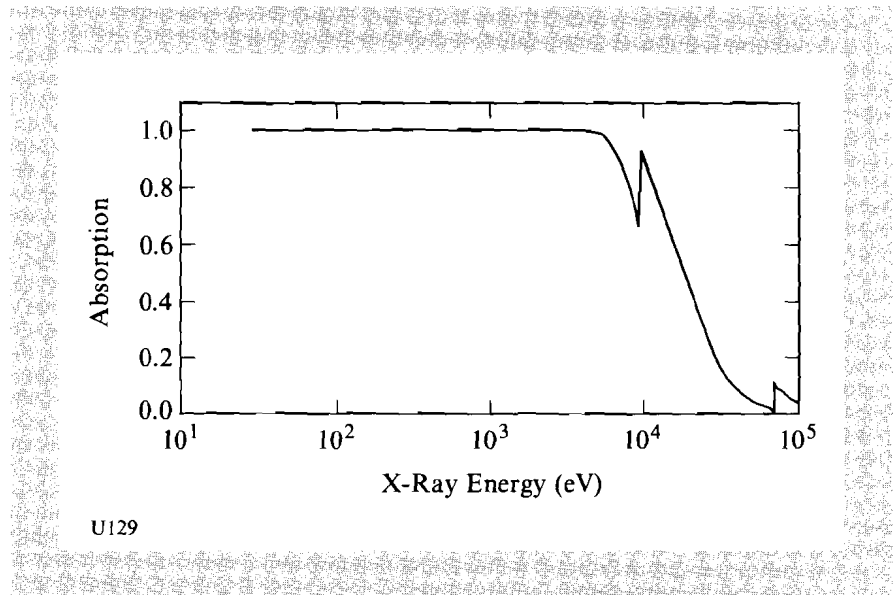
Fig. 31.8
X-ray calorimeter sensitivity.

electrons that radiate x rays with energies above 20 keV. The predominant contribution in the x-ray spectrum will come from silicon line emission and the low-energy continuum.

With the increased efficiency of energy absorption of targets when irradiated with shorter-wavelength lasers, the emission of soft x rays by the overdense plasma needs to be characterized. Figure 31.9 shows the percent of absorbed energy radiated into x rays as a function of incident-laser intensity for solid glass spheres. The circular points are the measured data and the square points are the predicted *LILAC* values for the experimental parameters. It is evident that there is good agreement between the experimental measurements and the theoretical calculations over the incident intensities from 6×10^{13} to 2×10^{15} W/cm^2. At these intensities, about 20% of the absorbed energy is converted to x rays.

X-ray radiation in *LILAC* is calculated with a multigroup line model. The group elements have been optimized for the hydrogen-like and helium-like lines in the silicon emission spectrum. The radiation transport is then done with the assumption of local thermodynamic equilibrium and look-up tables for the opacities. This calculation works well at predicting the x-ray fluence over a broad range of laser intensities.

The agreement between the *LILAC* calculations and the experimental measurements for solid glass targets is very good. The experiments have studied the coronal region of the plasma, where the majority of the laser energy is absorbed and where most of the line emission originates. The agreement between the calculations and the measured data indicate that the physics of the plasma corona is well understood. Since these are solid targets, the experiments are not complicated by the motion of the target surface. Thus, the plasma establishes a set of physical conditions that are relatively stationary and can be well modeled. Figure 31.10 shows that a stationary target surface is not
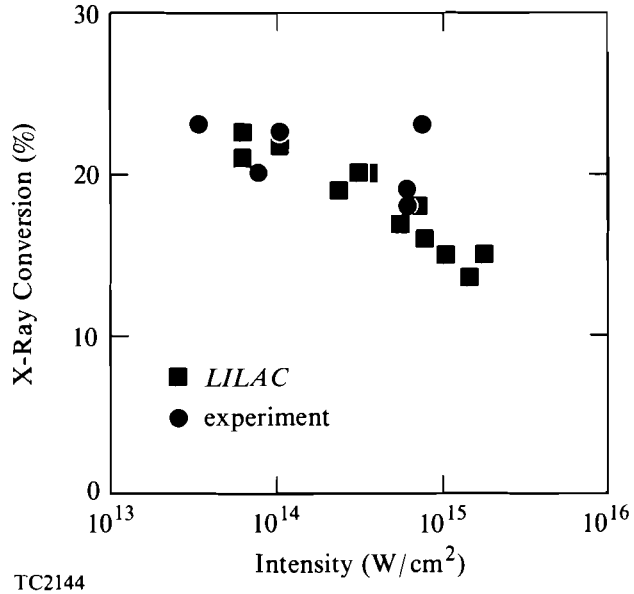
Fig. 31.9
Solid glass targets: x-ray conversion efficiency.
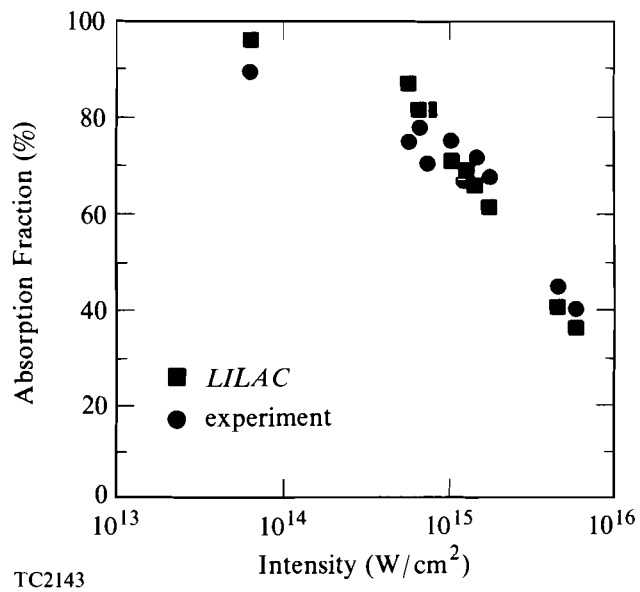
Fig. 31.10
Glass shell targets: absorption.

necessary for *LILAC* to predict measured absorption correctly. The absorbed energy fraction is plotted versus incident laser intensity. The round points are the experimental data and the square points are the *LILAC* predictions. The agreement is quite good and confirms that the coronal conditions of the laser-generated plasma are well understood in terms of the absorption of incident energy and the radiation of this energy into x rays.